International Journal of Rotating Machinery, 10(4): 283–291, 2004

ISSN: 1023-621X print / 1542-3034 online
DOI: 10.1080/10236210490447728

Taylor & Francis
Taylor & Francis Group

Deflections and Strains in Cracked Shafts due to Rotating Loads: A Numerical and Experimental Analysis

N. Bachschmid and E. Tanzi
Dipartimento di Meccanica, Politecnico di Milano, Milano, Italy

In this article, the deflections of a circular cross-section beam presenting a transverse crack of different depths, due to different loads (bending, torsion, shear, and axial loads), are analyzed with the aid of a rather refined 3-D model, which takes into account the nonlinear contact forces in the cracked area. The bending and shear loads are applied in several different angular positions, in order to simulate a rotating load on a fixed beam, or, by changing the reference system, a fixed load on a rotating beam. Torsion and axial loads are instead fixed with respect to the beam.

Results obtained for the rotating beam can then be used for the analysis of cracked, horizontal axis heavy rotors, in which the torsion is combined to the bending load. The effect of friction is also considered in the cracked area. The characteristic "breathing" behavior of the cracked area has been analyzed and compared to that one obtained with a rather simple 1-D model. The differences in results with respect to those which can be obtained by means of the approach based on fracture mechanics are emphasized.

In order to highlight the effect of the presence of the crack, the deflections of the uncracked beam loaded with the same loads are subtracted from the deflections of the cracked beam.

Finally, a cracked specimen has been extensively analyzed by means of several strain gauges, for analyzing the strain distribution on the outer surface around the crack, in different loading conditions. Consistent pre-stresses have been found, which influence the breathing behavior. The experimental results have been compared to those obtained with the 1-D linear model.

Received 25 June 2002; accepted 1 July 2002.
Address correspondence to N. Bachschmid, Dipartimento di Meccanica, Politecnico di Milano, Via La Masa 34, I-20158 Milano, Italy. E-mail: nicolo.bachschmid@polimi.it

Keywords Cracks, Shafts

The behavior of a crack in a rotating shaft can be modeled by different methods as reported in previous literature. In this work, an original simplified linear model that allows cracks of different shape to be modeled is used for calculating deflections of cracked beams in different loading conditions. The results are compared to those obtained with other methods: a cumbersome 3-D nonlinear finite element (F.E.) model and a model obtained through the strain energy release rate approach from fracture mechanics. The comparison allows one to evaluate the accuracy of the methods with respect to the 3-D model. Finally, some experimental results obtained on a cracked specimen show some unexpected effects, which can also easily be simulated by the simplified model.

TEST BEAM DESCRIPTION

The test beam used for the validation is a circular cross-section beam with diameter $d = 25$ mm and length $l = 50$ mm, with a crack of different shapes in the middle. The beam is represented in Figure 1 together with the reference frame according to which the deflections are evaluated. The beam is clamped at one end and a bending moment of $M_b = 10$ Nm and a torsion of $M_t = 25$ Nm have been applied to the other end. Also, a shear force T of 1000 N has been applied in some cases at the free end of the clamped beam, to investigate its effects and an axial force N of 1500 N in some other cases. Deflections have been evaluated at the same end of the beam. In the 3-D model, in order to avoid local deformations in the section where deflections are evaluated, the beam has an extension, and the loads are applied to the end of this extension. The bending moment is then rotated in the direction of Ω.

DESCRIPTION OF THE MODEL

The deflections of a test specimen are calculated by means of three different models.

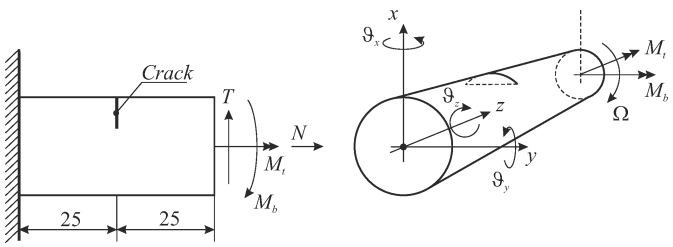

FIGURE 1
Test beam.

1. A 3-D finite element model.
2. A model based on fracture mechanics approach.
3. The simplified 1-D model developed by the authors.

THE 3-D MODEL

Figures 2 and 3 show the mesh which has been used for the cracked cylinder, with a relative crack depth of 25% and 50%. Roughly 9000 and 11000 elements, respectively, have been used for the analysis of the two cracked cylindrical beams. The mesh has been chosen rather "dense" because not only deformations of the cracked specimen, but also stress intensity factors in correspondence of the crack tip have been calculated numerically and compared with those calculated by means of the classical fracture mechanics approach. This comparison allowed the evaluation of the accuracy of the model in regards to its capability of representing real crack behavior in the region close to the crack. The elastic limit was never exceeded in the simulations.

The contact model in the cracked surface is obviously nonlinear. Also, a friction coefficient ($f = 0.2$) has been introduced in order to account for microslip conditions in the cracked area, due to shear forces and torsion. In order to avoid local deformations due to the application of loads, the model has been extended to a higher length where a pure bending load is applied to the specimen. This way in the cracked area and in the "measuring" section, where the deflections are evaluated and indicated by the dashed line, no local deformations are present, due to the application of loads. The results obtained with this model will be called simply 3-D results.

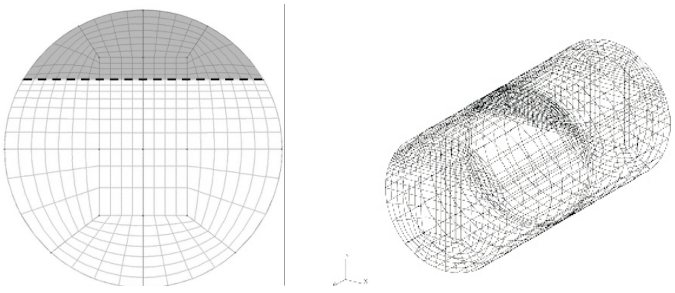

(a) (b)

FIGURE 2
Mesh of the section and isometric view of the model with a crack of 25%. The crack tip is indicated by the dashed line.

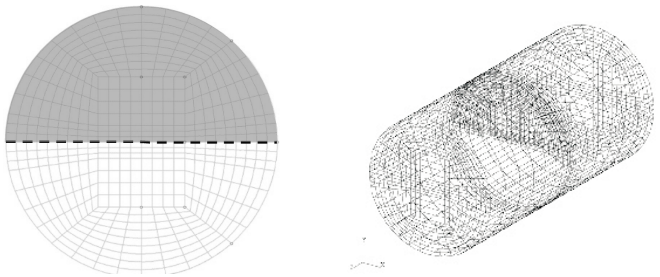

(a) (b)

FIGURE 3
Mesh of the section and isometric view of the model with a crack of 50%. The crack tip is indicated by the dashed line.

THE SERR MODEL

Since the *strain energy release rate* (SERR) approach combined with the stress intensity factors (SIF) had been used by many authors (as shown in [1], [2], and [3]) for the calculations of the cracked beam bending behavior, several calculations according to this approach and for different crack depths have been made. In this case, the "breathing" mechanism was assumed to be known (from Finite Elements Method or from simplified model) and the SERR approach was applied to the cracked cross section, with its open and close portions, in order to calculate the beam bending stiffness, as described in detail in [4]. The extension of this approach to the breathing crack is affected by some errors due to the fact that the crack tip is supposed to be formed by the boundary between the cracked areas and the uncracked areas for the regions in which the breathing crack is "open," which is correct, and by the boundary between the "closed" cracked areas and the "open" cracked areas, which is not correct because on this boundary no stress intensity factors will appear.

The traditional approach is relatively simple and the nodal-type model allows the local character of the crack to be considered. The values of the terms of the stiffness matrix of the crack element depend on the open or closed configuration of the crack which can be evaluated by testing the sign of the product of the relative displacement vector of the two nodes of the crack by the position vector of the crack, that is the normal vector at the crack face and oriented towards the open part. This approach is very useful to evaluate the stress distribution in the cracked section however, it does not consider the effects of the thermal stress on the breathing mechanism of the crack and the breathing itself is only roughly estimated as the crack is considered completely open or closed. As far as the authors know, the breathing mechanism has been simulated in previous studies by assigning a pre-established analytical law of the stiffness variation

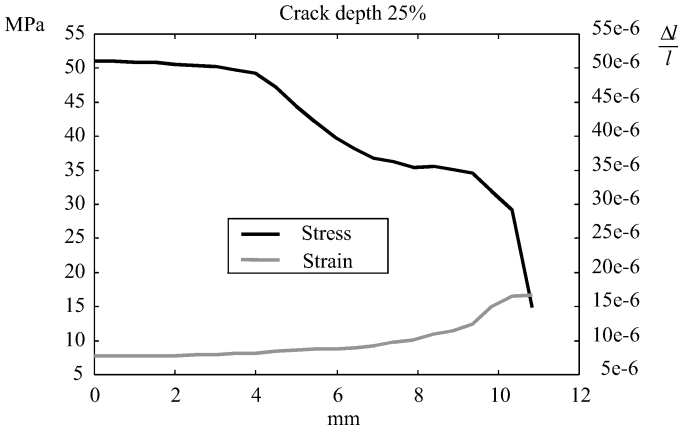

FIGURE 4
Distribution of strains and stresses along the tip of a 25% depth crack.

over the rotation. In this investigation, the nodal-type model approach combined with other crack models that take into account the breathing mechanism, has been used for obtaining results to be compared with cumbersome 3-D calculations and with the results of the simplified model.

This approach assumes stress and strain distributions with same values along directions parallel to the applied bending moment axis (as they are in rectangular cross sections), and no collaboration between parallel "rectangular slices" in which the circular cross section has been divided. This is not realistic, as it is shown in Figure 4, where stress and strain along the crack tip are shown, as a result of 3-D calculation. The cracked cross section is no longer planar, but distorted. This is not taken into account by the fracture mechanics approach.

The fracture mechanics approach further does not consider any friction on the cracked area, and this also seems to be unrealistic. If torsion is present, the contribution of friction forces on the cracked area can be taken into account only by the nonlinear 3-D calculation, and in an approximate way, by the simplified model.

The results obtained with this model will be called SERR results.

THE 1-D FLEX MODEL

The crack model, which was already presented in [5], is composed of a simplified equivalent beam model and a simplified model of the breathing mechanism, as a function of the static bending moment stresses. In the points of the cracked area where the stresses are compressive, contact occurs between the two faces of the crack; where the stresses are instead tensile, no contact occurs. This way the open and closed parts of the cracked area are determined in the different angular positions. The procedure is obviously roughly approximated since the actual stress distribution over the cracked cross section due to bending moment is not at all linear (as assumed by the simplified model). The closed parts of the cracked area and the uncracked area contribute to the second moments of the area, which determines the stiffness of the equivalent beam, which is a function of the angular position of the rotor with respect to the fixed weight load.

THE BREATHING BEHAVIOR

The breathing mechanism is generated by the bending moment due to external loads, such as weight and bearing reaction forces. The bending moment of 10 Nm generates a maximum axial stress of 6.5 N/mm^2 on the outer cylinder surface. The breathing is produced by the stress distribution around the crack. Therefore the following question arises: Is the breathing influenced also by the shear stresses due to the external torsion moment, which certainly changes the stress distribution around the crack? To answer this question to the 3-D model of the cracked beam, a rather high torsion moment has been applied to emphasize this effect.

The torsion moment of Mt = 25 Nm generates a maximum tangential stress which is 1.25 times the maximum axial stress due to the bending moment of 10 Nm. Comparing the results obtained in the case of bending + torsion loading to those of pure bending loading, in the different angular positions it has been shown that the effect of torsion loads on the breathing mechanism of cracks can be neglected.

Even if the highly nonlinear stress distribution in the 3-D FEM is different from the linear one considered in the simplified model, the two models actually show a rather good agreement as regards to the "breathing" mechanism for both 25 and 50 percent depth crack.

The breathing behavior allows one to calculate the areas and the second moments of area of the cracked section which are used for calculating the stiffness of the cracked beam in the different angular positions. Applying different loads, the deflections can then be calculated.

DEFLECTIONS

In order to emphasize the additional deflections which are due to the presence of the crack alone, the deflections of the

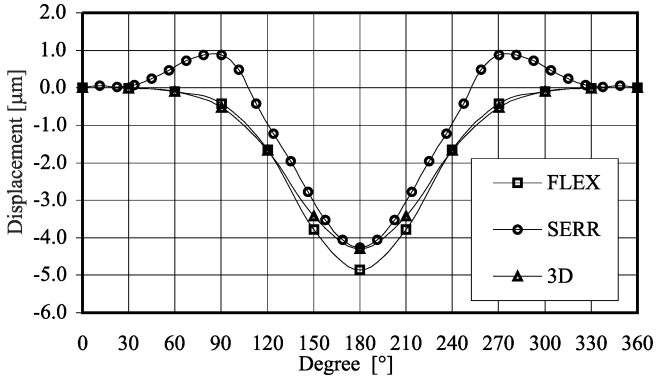

FIGURE 5
Pure bending, 50% crack depth, x displacement.

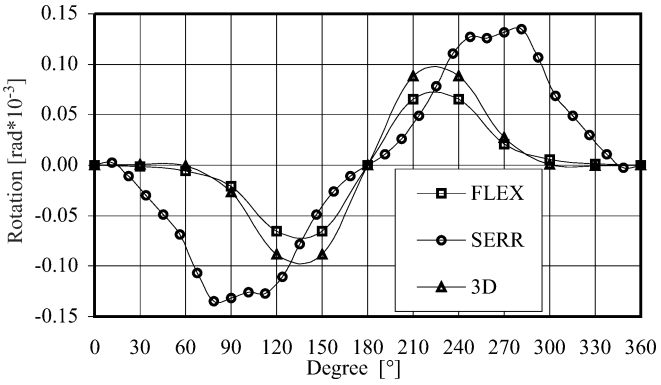

FIGURE 6
Pure bending, 50% crack depth, ϑ_x rotation.

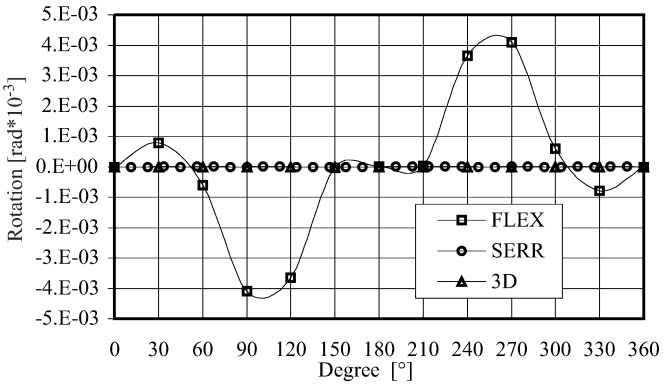

FIGURE 8
Pure bending, 50% crack depth, ϑ_z rotation.

cracked specimen have been compared to the deflections of the uncracked specimen, and its differences have been extracted. This procedure allows one also to appreciate small differences in behavior due to the different modeling methods of the crack.

The deflections are calculated in the center of the circular end cross section of the specimen modeled with finite beam elements, according to the FLEX model and the SERR model derived from fracture mechanics. All six components of the deflection have been calculated for the different angular positions of the load with respect to the crack, obtained by increasing the angle by steps of 30°.

Two different crack shapes have been considered: rectilinear crack with a relative depth of 25 percent and rectilinear crack with a relative depth of 50 percent. Different loads (bending, shear, torsion, and axial loads) have been applied to the same specimen in order to simulate all possible loads in rotating shafts in operation. Finally, all results have been compared. In the following some of the obtained results are shown.

PURE BENDING

From Figures 5 and 6 it can be seen that the FLEX model results are rather close to the 3-D results, closer than the SERR results. Similar behaviors have been found for the other degrees of freedom y and ϑ_y. Only the axial displacement, z (Figure 7), due to coupling effects is underestimated and the torsional deflection (Figure 8) due to coupling effects is overestimated by the FLEX model. However, the differences (errors) are so small, with respect to the other deflections, that they can be neglected. Similar results also have been found for the 25 percent deep crack.

BENDING AND TORSION

Due to the presence of torsion, the diagrams are no longer symmetrical in general. Again the FLEX results are closer to 3-D results, with respect to SERR results as shown in Figures 9 and 10. In particular, the torsional flexibility is completely underestimated by SERR as shown in Figure 11. The axial displacement (not shown) seems unaffected by torsional loads and is exactly equal to the pure bending case.

BENDING AND SHEAR

The presence of shear forces lowers a little of the accuracy of the FLEX model in general, except for the axial displacement, with respect to the pure bending situation (see Figures 12

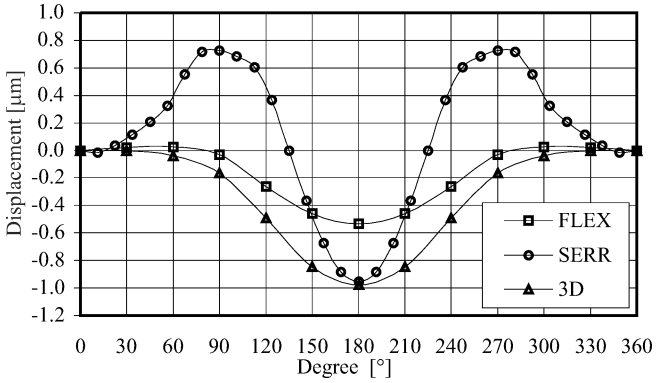

FIGURE 7
Pure bending, 50% crack depth, z displacement.

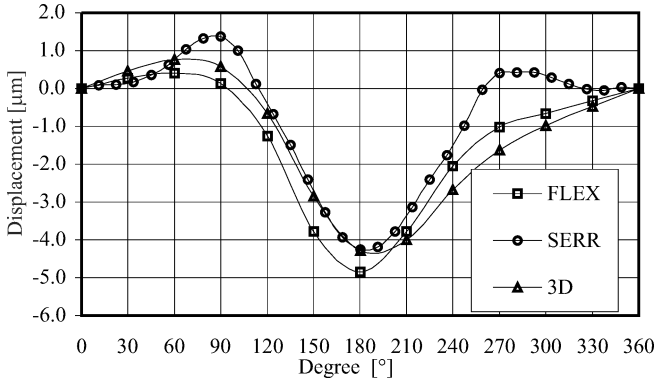

FIGURE 9
Bending and torsion, 50% crack depth, x displacement.

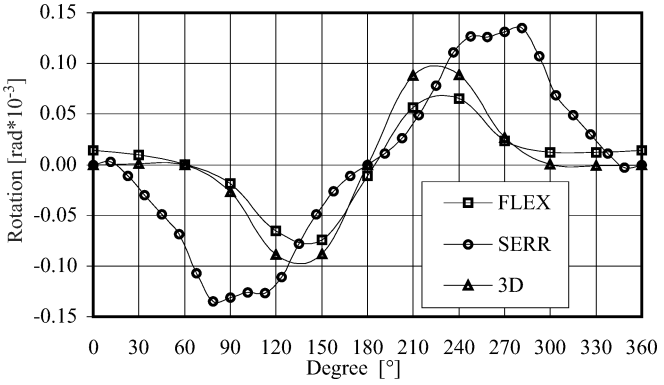

FIGURE 10
Bending and torsion, 50% crack depth, ϑ_x rotation.

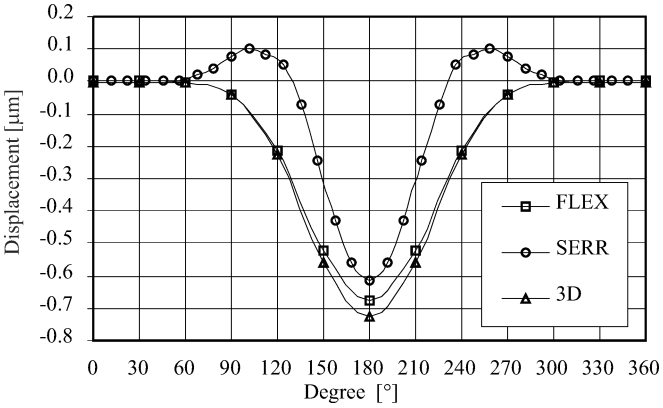

FIGURE 12
Bending and shear, 50% crack depth, x displacement.

and 13). It seems that the accuracy of the FLEX model is rather high, with few exceptions (as for the axial displacement).

AXIAL LOADS

Regarding the axial load as shown in Figures 14, 15, and 16, good agreement is found for horizontal and vertical displacements, which are due to coupling coefficients. The axial displacement is affected by an error of 6 percent, which seems acceptable. The error in torsional deflections are negligible, while the comparison with SERR results is not shown, because they seem unreasonable.

EXPERIMENTAL RESULTS

The results of a series of experimental tests performed on a cracked specimen in different loading conditions are described. These tests have been performed in the frame of common research activity with EDF (Electricité de France) on cracked rotors, and the cracked specimen was prepared by Centre Technique Industries Mecaniques, France (CETIM). The aim of the tests was to investigate the breathing behavior of the crack. In the vicinity of the crack lips, strain gauges have been applied in order to measure the stresses and identify the load conditions (the value of the bending moment and the angular position of the load with respect to the crack) in which the lips start to loose contact. The measured stresses have been finally compared to the stresses which are calculated through the simplified 1-D model.

DESCRIPTION OF THE TEST-RIG

The test specimen, schematically represented in Figure 17, has been bolted to a shaft extension mounted on two roller bearings in a supporting structure. The shaft is then held by a pin in different angular positions.

At the opposite specimen end several disks can be bolted to the end flange. In this way different bending moments are applied to the cracked specimen. Section A is the cracked section. The crack profile, as obtained by means of US tests is shown in Figure 18. Section B, being at a distance from the crack higher than the diameter of the specimen, is unaffected by the crack and is the reference section. Sixteen different strain gauges have been applied in the positions shown in Figure 18.

The strain gauges from SG1 to SG11 have been applied in correspondence of the crack lips, SG16 is in the position opposite

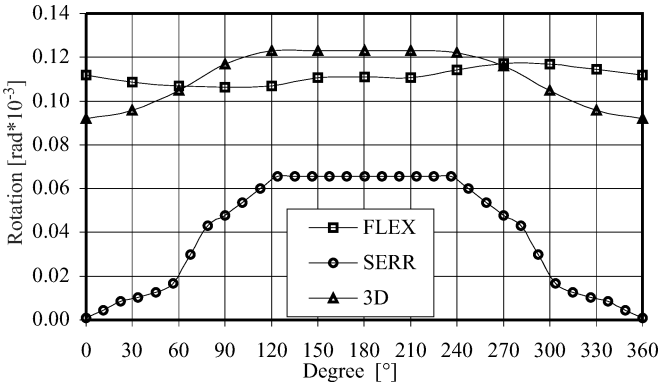

FIGURE 11
Bending and torsion, 50% crack depth, ϑ_z rotation.

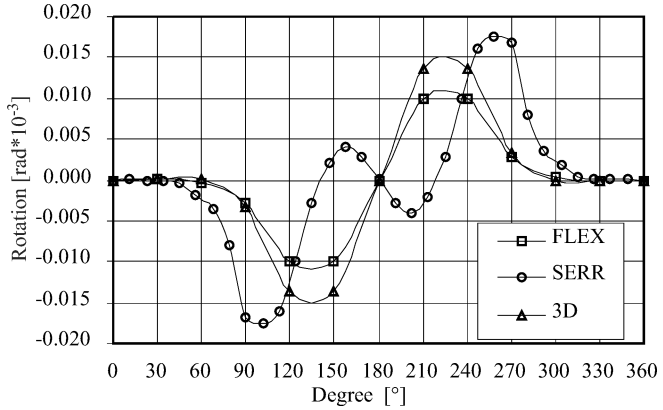

FIGURE 13
Bending and shear, 50% crack depth, ϑ_x rotation.

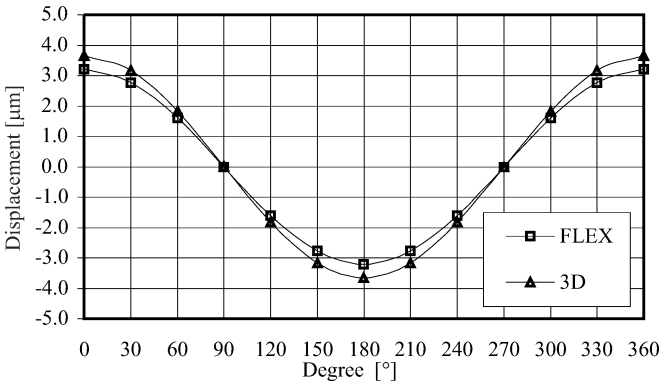

FIGURE 14
Axial load, 50% crack depth, x displacement.

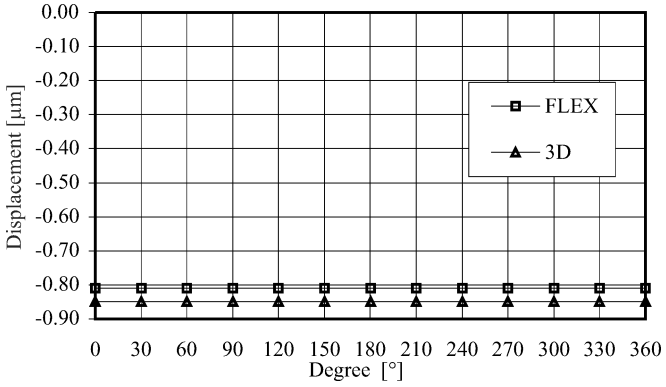

FIGURE 16
Axial load, 50% crack depth, *z* displacement.

to the crack lips in Section A, and SG12 and SG15 have been applied for reference on Section B.

MEASURED STRAINS

Strain gauge measurement results obtained for the different strain gauges, for the four different load conditions in the different angular positions (every 15°) of the cracked specimen with respect to the vertical load direction, are presented.

In the diagrams of Figures 19 to 23 the strains versus the rotation angle from 0 to 360° for the five different strain gauges applied to the cracked specimen in the positions shown in Figure 18, are represented. The different loading conditions are specified in the diagrams.

The initial position (0°) corresponds to the crack axis in vertical position. With the lower loads (from 0 M up to 3 M) the pure sinusoidal behavior of all strain gauges indicate that the crack is always closed. The positive strain on the crack lips (elongation) is probably an "apparent" relative strain (and not an absolute strain which, according also to 3-D calculations cannot be positive). The strain gauges have been applied to the specimen in a condition of external loads as close as possible to zero, but probably an internal bending moment has developed during the propagation of the crack, which tends to hold the crack closed. The crack lips are pressed against each other, so that, with no external loads, a compressive strain developes on the lips, which is not measured by the strain gauges. The crack lips open then only when the external bending moment overcomes the internal bending moment, and when the tensile stress due to the external load equals the compressive stress due to the internal bending moment. From this position on, the strain indicated by the gage, which is the relative strain with respect to the initial reference situation, should remain constant at the increasing of the load. From this position on, the absolute strain should be zero.

This condition is fulfilled only with the highest load (3M) and only for the gauges SG4, SG5, SG6, and SG7. In these measuring points the crack lips open completely in several different angular postions. In the other measuring points on the crack lips, or close to the crack lips, the strains always indicate closed crack condition, probably because these points are rather close to the crack tip, or slightly outside the crack lips.

Another interesting point can be stressed from these diagrams. The theoretical strain variation with maximum load, as shown in Table 1, is roughly between +40 and −40 microstrains in correspondence to Section A, with a total peak to peak variation of 80 microstrains. In measuring point SG16 we have a minimum of 55 microstrains, in the position where the crack is open, and the stress distribution is not linear, and a maximum

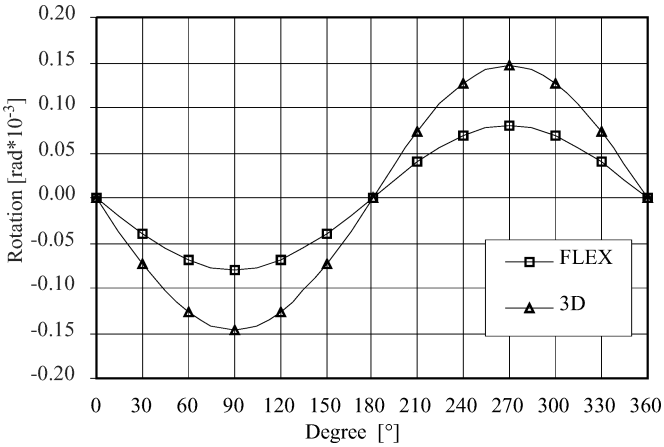

FIGURE 15
Axial load, 50% crack depth, ϑ_x rotation.

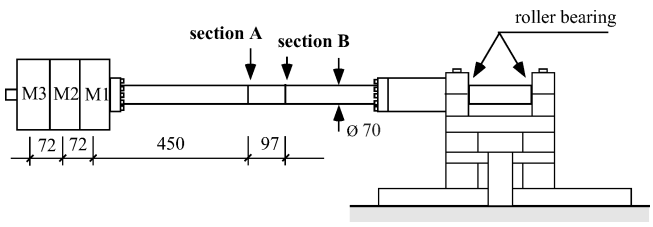

FIGURE 17
Schematic drawing of the test-rig (dimensions are in mm).

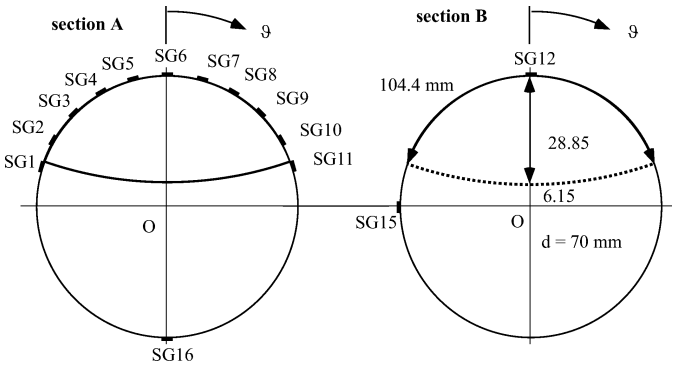

FIGURE 18
Strain gauge positions.

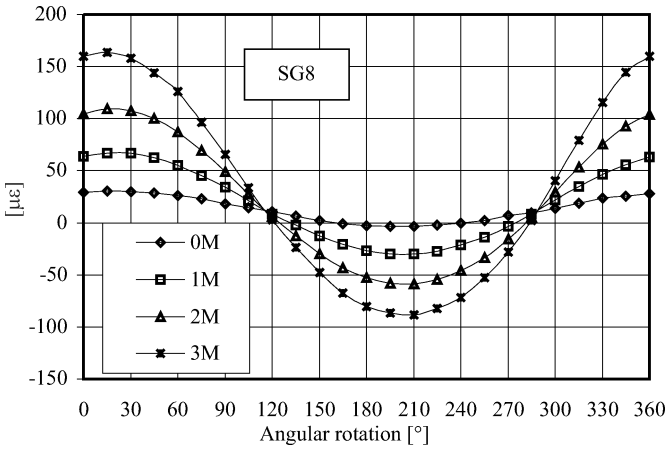

FIGURE 21
Strain gauge 8: strain versus rotation.

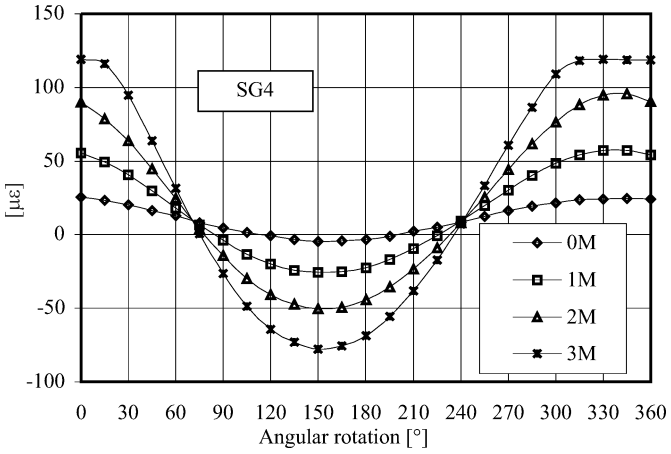

FIGURE 19
Strain gauge 4: strain versus rotation.

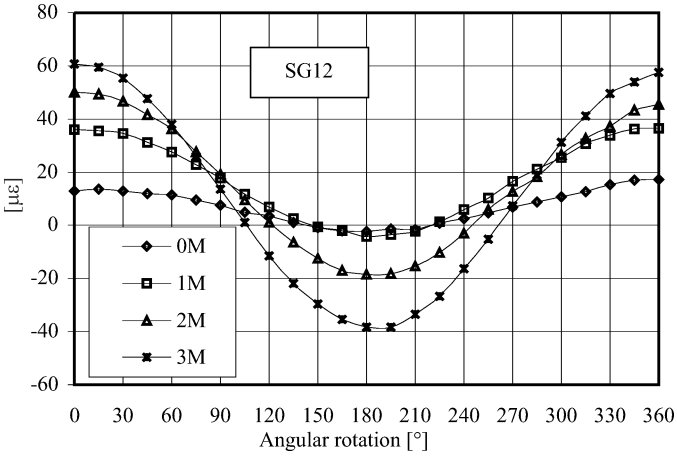

FIGURE 22
Strain gauge 12: strain versus rotation.

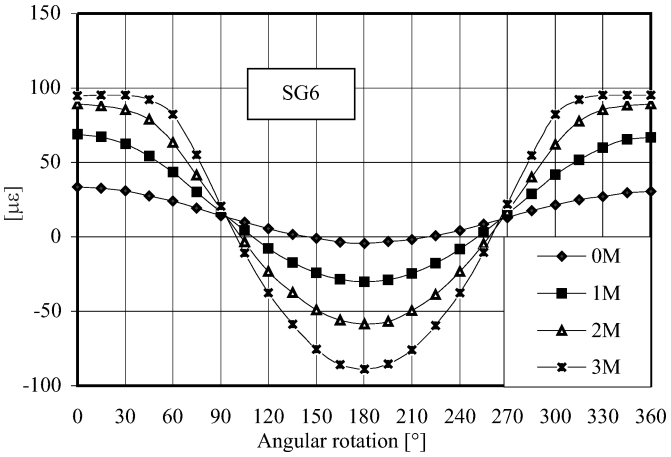

FIGURE 20
Strain gauge 6: strain versus rotation.

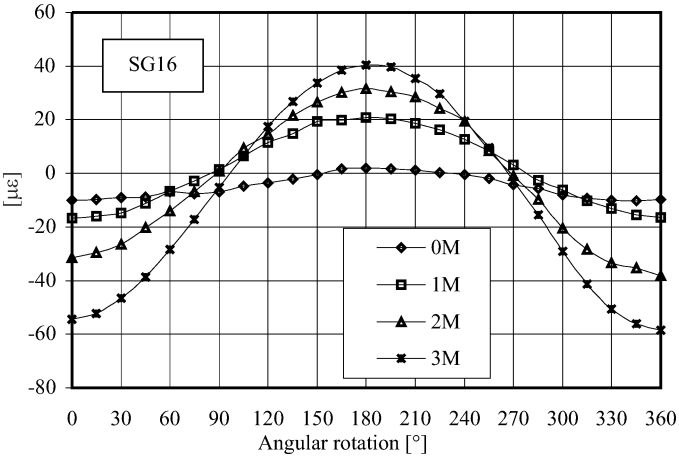

FIGURE 23
Strain gauge 16: strain versus rotation.

TABLE 1
Loads, bending moments (B.M.), and theoretical strains

	Section A			Section B		
Loads	B.M. [Nm]	σ [MPa]	ε [$\mu\varepsilon$]	B.M. [Nm]	σ [MPa]	ε [$\mu\varepsilon$]
0M	37.4	1.1	5.4	53.0	1.6	7.6
1M	104.4	3.1	15.1	134.8	4.0	19.4
2M	181.9	5.4	26.2	226.4	6.7	32.6
3M	270.7	8.0	39.0	329.7	9.7	47.5

0M: means no additional mass. 1M: means 1 additional mass. 2M: means 2 additional masses. 3M: means 3 additional masses.

of 40 microstrains, in the position where the crack is closed and the stress distribution should be linear. This last value is exactly the theoretical value.

In SG11 a total variation of 88 microstrains indicates no nonlinear effects; the crack does not open and in this position no stress concentration occurs. In SG1 a total variation of 130 microstrains indicates incoming nonlinear effects, which increase by moving towards the crack axis, on both sides. In SG10 and SG2, 150 microstrains exist, in SG3 there are 180 microstrains, and in SG8 and SG9 250 microstrain peak to peak variations are measured. In SG4 and SG5 the positive peak is flattened due to crack opening, and the minimum is -75 microstrains. Similar behavior is found in SG6 and SG7 where a minimum of -90 microstrains is reached.

The consistent increase of strains with respect to the theoretical values can be attributed to local stress concentration factors, which obviously depend on the different depths of the lip contact areas in correspondence to the different positions.

Finally, Figure 24 shows the calculated stress distribution for the 50 percent deep crack in case of open and closed cracks. As can be seen, in the case of closed crack, with flat crack surfaces, a linear stress distribution is obtained with no stress concentration effects.

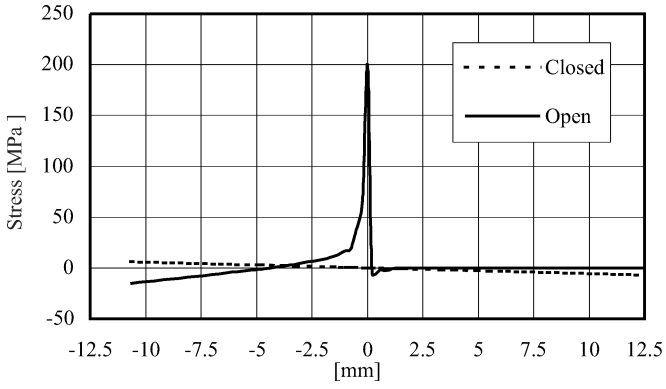

FIGURE 24
Calculated axial stress distribution for the 50% deep crack in case of open and closed crack.

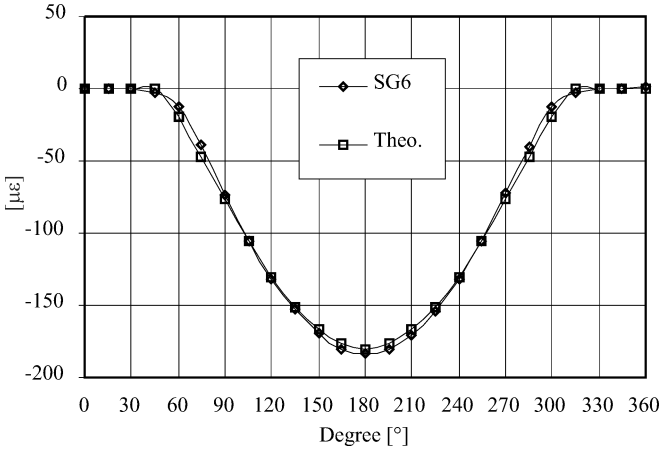

FIGURE 25
Theoretical strain values compared with measured strains in position SG6.

COMPARISON WITH THE SIMPLIFIED 1-D MODEL

The decribed 1-D model has been used to check its suitability for simulating the measured experimental results. The simplified model does not allow one to account for an internal preload in the cracked area, nor for a contact occurring only on the lips of the crack (and not on its total cracked area). However, an external bending moment which prevents the opening of the crack can be applied. This has been done, and the value of the bending moment has been tuned in order to have, with the maximum load applied to the specimen, the same angular positions in which the crack starts to open in the position of SG6. The calculated theoretical stress does not take into account any stress concentration factor which in this particular case could be rather high, because probably when the lips are closed, the contact occurs only in a small area below the outer surface of the lips.

With a stress concentration factor of 2.5 and a bending moment of -230 Nm the values shown in Figure 25 are obtained. They are compared with the values measured by SG6, which were shifted in order to have zero strain for open crack.

The excellent agreement between measured and calculated results, although obtained after tuning the zero position and the stress concentration factor, confirms once again the validity of the proposed simplified 1-D model.

CONCLUSIONS

Deflections of cracked beams according to 6 degrees of freedom (d.o.f.) due to different loading conditions have been calculated with three different methods and have been compared. The proposed linear 1-D model shows good agreement with the nonlinear 3-D model, both in the breathing behaviors (which influence the variation of the stiffness of the beam) and in

evaluating deflections. It is worth nothing that the analysis of each loading condition requires several hours of computation with the 3-D nonlinear model and only a few seconds with the 1-D model. The breathing behavior has finally been investigated experimentally and some interesting effects deriving from crack propagation have been discovered.

ACKNOWLEDGMENTS

The financial support of MURST cofinanziamento "Identificazione di malfunzionamenti nei sistemi meccanici" (1999) is gratefully acknowledged.

REFERENCES

Gasch, R. 1993. A survey of the dynamic behaviour of a simple rotating shaft with a transverse crack. *Journal of Sound and Vibration* 160(2):131–332.

Wauer, J. 1990. On the dynamics of cracked rotors: a literature survey. *Applied Mechanics Reviews* 43(1):13–17.

Dimarogonas, A. D. 1996. Vibration of cracked structures. A state of the art review. *Engineering Fracture Mechanics* 55:831–857.

Ferrari, G., and Campana, S. 1999. Comportamento statico e dinamico di un rotore criccato. Masters thesis, Politecnico di Milano.

Bachschmid, N., Vania, A., and Audebert, S. 2000. A Comparison of different methods for transverse crack modelling in rotor systems *ISROMAC 8*, March, 36-30, Honolulu, Hawaii.